QRS detection for pacemakers in a noisy environment using a time lagged artificial neural network

Rodrigues, Joachim; Öwall, Viktor; Sörnmo, Leif

Published in:
[Host publication title missing]

DOI:
10.1109/ISCAS.2001.921381

Published: 2001-01-01

QRS Detection for Pacemakers in a Noisy Environment Using a Time Lagged Artificial Neural Network

J. Neves Rodrigues, V. Öwall, and L. Sörnmo

Department of Electroscience, Lund University
Box 118, SE-221 00 Lund
Sweden

ABSTRACT

A time lagged feedforward artificial neural network (TLFN) is used to detect QRS complexes for pacemakers in a noisy environment. The TLFN reduces the influence of lower frequencies in the invasive electrogram (EG) signals, such as the P and T waves. The TLFN output is then subjected to matched filtering with a dynamically updated impulse response. Detector performance is studied by means of databases containing electrograms and noise such that different types of noise and interferences from electronic appliances are added to the electrograms. Results show that the detector performs well in many different noisy environments by considerably improving the signal-to-noise ratio (SNR).

1. INTRODUCTION

The electromagnetic radiation due to electronic appliances has increased dramatically during the last decades, e.g., from electronic household devices or electronic article surveillance systems. Pacemakers of today may suffer a considerable degradation in performance under such circumstances. In particular, the number of falsely detected QRS complexes will increase due to a poor SNR and cause the pacemaker to switch to permanent pacing, regardless of the heart rate of the patient. Such a mode shortens the lifetime of the pacemaker due to a higher power dissipation. Another drawback for the patient is that this mode may cause hypertrophy of the heart in the long run.

Current pacemaker detectors typically include a bandpass filter in combination with a fixed threshold procedure for finding the cardiac events. Unfortunately, the "optimal" passband differs not only from patient to patient but may change over time within the same patient. If the electrogram is heavily corrupted with noise, detection performance will drop even further. Hence, robustness against electromagnetic radiation becomes a major design constraint for algorithms to be implemented in a pacemaker. A major motivation for our research is therefore to find such robust algorithms that are suitable for an implementation in low power digital ASIC.

2. METHODS

To overcome the problem of defining a suitable filter passband, a TLFN is applied as an adaptive filter [1], [2]. Additionally, a dynamically updated matched filter is used in order to maximize the QRS amplitude in a noisy environment. Finally, an adaptive threshold is used to decide whether or not a QRS has occurred and, eventually, to cause an update of the template for the matched filter, as shown in Figure 1. Without any QRS complex detection within a certain time range, the pulse generator is alerted to send out an artificial pacing impulse.

3. THEORY

The TLFN is a supervised network which acts like a one-step predictor of the current sample using the immediately preceding samples ("whitening filter") [2]. The over-all behavior of the network is primarily to predict lower frequencies contained in the electrogram. The occurrence of a QRS complex, which is associated with a higher frequency content, implies that the prediction error will suddenly increase, and, accordingly, indicate the presence of a QRS.

The TLFN consists of a forward and a backward pass, as shown in Figure 2. In the forward pass, the stimulus (input) is propagated rightwards through the entire network in order to produce a prediction. The error between such a prediction and the desired response is then propagated backwards in order to update the synaptic weights. This procedure is referred to as the training of the network. All the free adjustable synaptic weights, $w(n)$, are updated in order to minimize the error with a least mean square (LMS) algorithm [1].

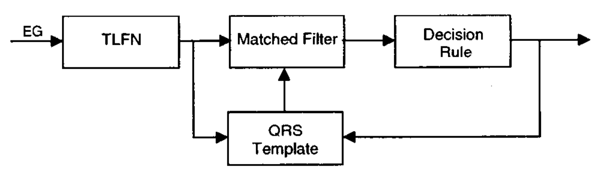

Figure 1. Block diagram of the detection algorithm.

3.1 Forward pass

The applied TLFN has M input nodes, according to M preceding samples for the prediction, L nodes in a hidden layer and $(M+2)L+1$ synaptic weights, $w(n)$, as shown in Figure 2. Each node is consists of a summation point, an externally applied bias connected to an input fixed at +1, and a nonlinear activation or threshold function φ. The most common applied activation function also used in this network, is the hyperbolic tangent function, which is a graceful balance between linear and nonlinear behavior [1].

0-7803-6685-9/01/$10.00©2001 IEEE

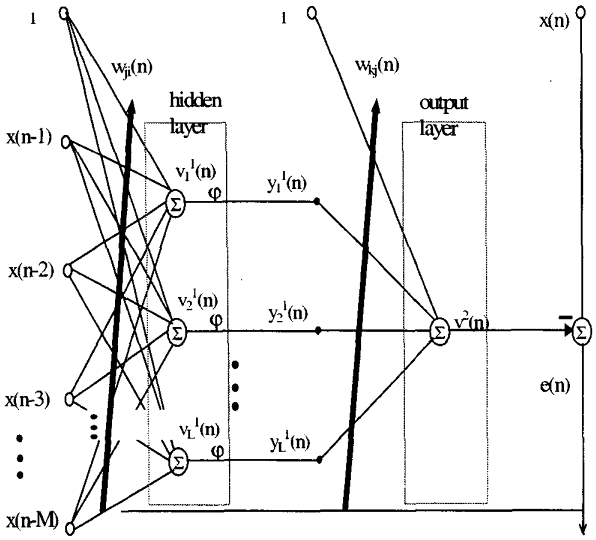

Figure 2. The Time Lagged Feedforward Neural Network

The output vector $\mathbf{v}^{(1)}$ of the summation nodes in the hidden layer is calculated as

$$\mathbf{v}^{(1)} = \mathbf{W}^{(1)}\mathbf{x}(n)$$

$$\begin{bmatrix} v_1^{(1)}(n) \\ v_2^{(1)}(n) \\ \vdots \\ v_L^{(1)}(n) \end{bmatrix} = \begin{bmatrix} w_{10}^{(1)}(n) & w_{11}^{(1)}(n) & \cdots & w_{1M}^{(1)}(n) \\ w_{20}^{(1)}(n) & w_{21}^{(1)}(n) & \cdots & w_{2M}^{(1)}(n) \\ \vdots & \vdots & \ddots & \vdots \\ w_{L0}^{(1)}(n) & w_{L1}^{(1)}(n) & \cdots & w_{LM}^{(1)}(n) \end{bmatrix} \begin{bmatrix} 1 \\ x_1(n-1) \\ \vdots \\ x_4(n-M) \end{bmatrix} \quad (1)$$

with M=4 and L=3. Thereafter, the output $\mathbf{v}^{(1)}$ is further processed with the nonlinear activation function according to

$$\mathbf{y}^{(1)}(n) = \varphi\left(\mathbf{v}^{(1)}(n)\right), \quad (2)$$

which is the output of the hidden layer. Such an output of the hidden layer, according to (2), is propagated further to the next layer. Since the network only has one hidden layer the next layer is the output layer. The output layer consists of a single node. Thus the response of the network is calculated as

$$v_1^{(2)}(n) = \mathbf{W}^{(2)}\left[1 \quad \mathbf{y}^{(1)}\right]^T. \quad (3)$$

As shown in (3) the output of the network is the weighted and summed response of the hidden layer.

3.2 Back-propagation pass

In the back-propagation pass all the synaptic weights, $w(n)$, are updated with the well known back-propagation algorithm [1]. The objective of the back-propagation algorithm is to train the network. This is done in order to minimize the deviation of the response to the desired prediction. Such a deviation (error) is defined as

$$e(n) = x(n) - v_1^{(2)}(n). \quad (4)$$

All the errors are squared and summed according to

$$\varepsilon(n) = \frac{1}{2}\sum_{j\in C} e_j^2(n), \quad (5)$$

where the set of C=1 includes all the neurons in the output layer. The error function is minimized with the use of the LMS algorithm [1] as

$$\begin{aligned} \frac{\delta\varepsilon(n)}{\delta w_{ji}(n)} &= \frac{\delta\varepsilon(n)}{\delta e_j(n)}\frac{\delta e_j(n)}{\delta y_j(n)}\frac{\delta y_j(n)}{\delta v_j(n)}\frac{\delta v_j(n)}{\delta w_j(n)} \\ &= -e_j(n)\varphi'\left(v_j(n)\right)y_i(n). \end{aligned} \quad (6)$$

The correction Δw_{ji} applied to the synaptic weights is performed with the delta rule according to

$$\Delta w_{ji}(n) = -\eta\frac{\delta\varepsilon(n)}{\delta w_{ji}(n)}, \quad (7)$$

where η is the learning rate. The negative sign in (7) is due to the gradient descent in weight space. Inserting (6) in (7) yields

$$\Delta w_{ji}(n) = \eta e_j(n)\varphi'\left(v_j(n)\right)y_i(n), \quad (8)$$

where φ' is the time derivative of the activation function. The learning speed is accelerated with the addition of a fraction, α, of the previous weight update to the current update. Moreover, the use of a momentum term α is a possibility to overcome the problem of getting stuck in a local minima. The weight updates for the hidden layer and the output layer are calculated according to

$$\Delta w_{ji}(n) = \eta e_j(n)\varphi'\left(v_j(n)\right)y_i(n) + \alpha\Delta w_{ji}(n-1) \quad (9)$$

and

$$\Delta w_{kj}(n) = \eta e_j(n)y_j(n) + \alpha\Delta w_{kj}(n-1). \quad (10)$$

Finally, all the free adjustable synaptic weights, $w(n)$, in the network are updated by adding (9) and (10) to the corresponding weights.

3.3 Matched Filtering

A matched filter is applied to the TLFN output to improve the SNR, see Figure 1. Assuming that the input signal is corrupted with white noise, it is well-known that the impulse response, $h(n)$, of the matched filter is a time-reversed replica of the event to be detected, i.e., the QRS complex, see Figure 3b. Such a template, $h(n)$, is generated automatically by monitoring the output of the TLFN. The output of the matched filter is obtained from a template with the length of twenty, (the sampling rate for the EG sample rate is 250 Hz) and then propagated further to the adaptive threshold function.

Such a threshold function uses the peak amplitude of the previous detected QRS complex in order to adapt the threshold. In the case of a detection, the template for the matched filter is updated according to

$$h(n) = \beta h(n-1) + (1-\beta)h(n), \quad (11)$$

where β in (11) is an update factor.

3.4 Signal and Noise Databases

The electrogram database contains 110 signals from different patients. The signals were recorded during pacemaker implantation in several hospitals using a digital mini disc (MD) unit at the input of a pacemaker. The pacemaker electrode is placed either in the right or the left atrium. A typical signal for a healthy person that was recorded at the end of the electrode is shown in Figure 3a. It can be seen that the P and T wave are inherently lower frequencies and the QRS has a higher frequency content.

The noise database has two different types of signals, endogenic and exogenic interferences. The endogenic signals are myopotentials caused by muscle contractions of the human body. The exogenic interferences are caused by sources such as a hand drill, hand mixer or electronic article surveillance (EAS) systems.

4. RESULTS

The performance of the detector is evaluated by adding different types of noise to the electrogram. However, for the first analysis an EG, which is not easy to classify, is filtered without adding any interference, see Figure 4a. The EG is heavily disturbed and represents a signal in which it is even visually difficult to find the QRS complexes. The signal in Figure 4a is passed through the TLFN in order to suppress the P and T waves and the output is shown in Figure 4b. Figure 4c shows the output of the matched filter, which is almost noise-free, and the QRS complexes can now easily be detected with the adaptive threshold function. The adaptive amplitude threshold function is set to 66% of the previous QRS amplitude. The crosses in Figure 4c indicate the detected QRS complexes. The true number of QRS's in the observed time period is 323, however, the detector found 324 events; two false alarms resulted and one QRS remained undetected.

In order to explore the detection performance in a very noise environment two different type of interferences were added to noise-free signals. The electrograms have been disturbed during two minutes. The first interference added to an EG is obtained from an electronic article surveillance system (EAS) as shown in Figure 5. In order to define a noise level, the standard deviation of a QRS template and the interference are equalized. In Figure 5a the noise-free EG is plotted, and Figure 5b shows the same EG but with added EAS interference. The output of the TLFN and the matched filter is shown in is in Figure 5c and Figure 5d, respectively. It can be seen that the SNR is significantly improved with the matched filter. The QRS's can be easily detected with the adaptive threshold. For the time period of interest 132 QRS's out of 136 are detected, without any false detections.

The next signal contains noise from a hand drill, see Figure 6. As shown in Figure 6d, the performance of the matched filter is not as good as in the previous example. Although the SNR is improved, the noise is not as well suppressed as in Figure 5. The true number of QRS's complexes is 120, however, 126 events were detected. Among these 126 detections, eight were falsely detected (one of these is pointed out in Figure 6 with the arrow), and two QRS's complexes were missed. A false detection is due to a peak that exceeds the threshold in a certain time period where a QRS complex is expected.

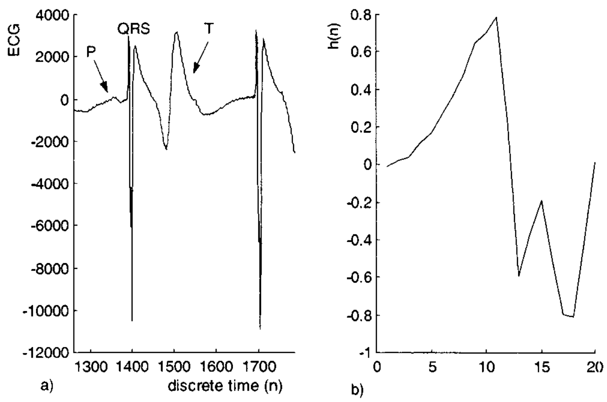

Figure 3 a) The noise-free EG from patient #3, with the P, QRS and T wave, respectively, b) a template $h(n)$ used for the matched filter.

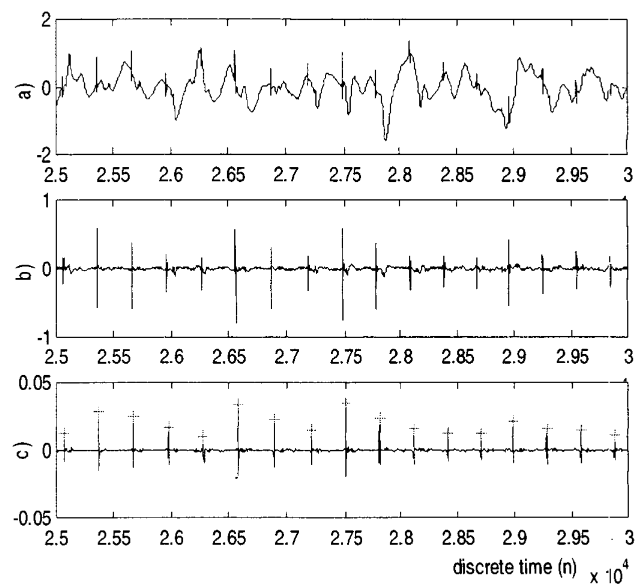

Figure 4 a) noise-free EG from patient #33, b) output of the TLFN, c) output of matched filter with indicated detections

5. CONCLUSIONS

The presented adaptive filter structure is tested on different patients with various types of noise and interferences. The filter adapts to different patients and their inherently time-varying EG properties. Hence, the filter performance does not depend on the particular properties of a patient. It is shown that the detector structure performs well in filtering out "physiological noise", i.e., the P and T wave. Moreover, the degradation in filtering performance is limited even if the EG is heavily interfered from external sources such as an EAS or a hand drill. Thus, detection performance is achievable even though the EG is heavily interfered. These results will finally lead to an implementation of the filter and detector structure in a low power digital ASIC suitable for the next generation of pacemakers.

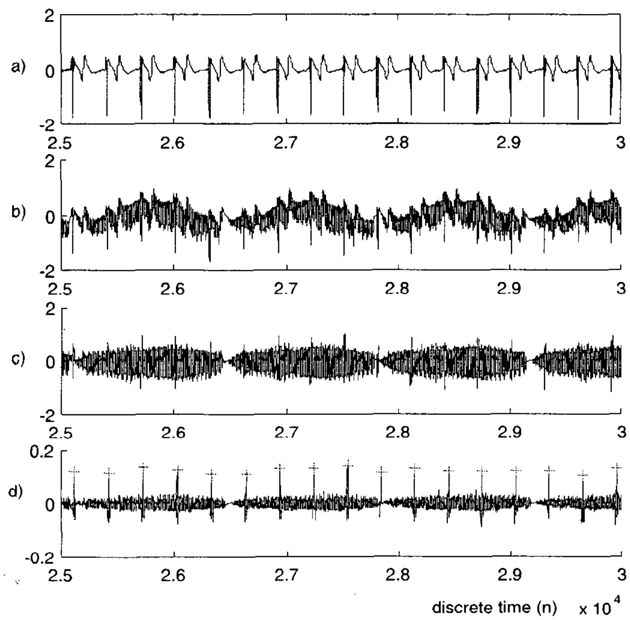

Figure 5 a) Noisefree EG from patient #3a, b) EG interfered with a noise from an EAS, c) output of the TLFN, d) signal after the matched filtering with indicated detections.

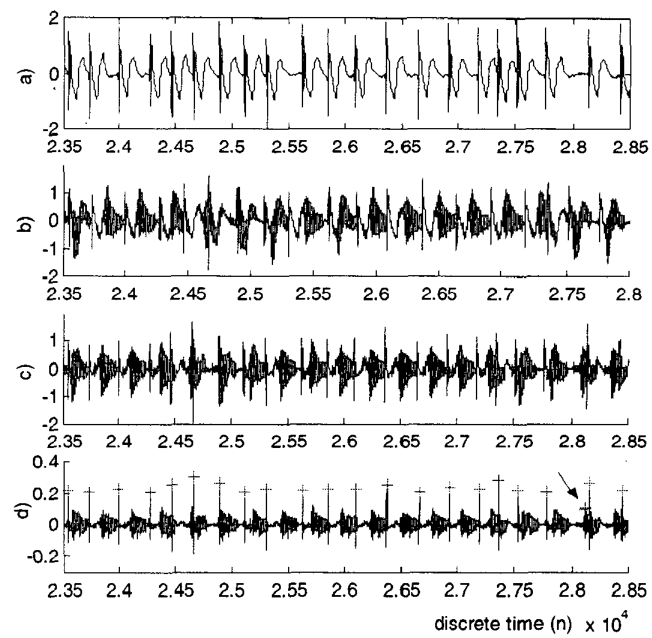

Figure 6 a) Noisefree EG from patient #10a, b) EG interfered with a noise from a hand drill, c) output of the TLFN, d) signal after the matched filtering with indicated detections.

6. REFERENCES

[1] S. Haykin, *Neural Networks, a comprehensive foundation*, Prentice Hall, 1999.

[2] Q. Xue, Y.H. Hu, W.J. Tompkins, "Neural-Network-Based Apative Matched Filtering for QRS detection". *IEEE Transactions on Biomedical Engineering*, April 1992, pages 317-328

[3] G.M. Friesen, T.C. Jannett, M.A. Jadallah, S.L Yates, S.R. Quint, H.T. Nagle, "A Comparison of the Noise Sensitivity of Nine QRS Detection Algorithms". *IEEE Transactions on Biomedical Engineering*, January 1990, pages 85-98.

[4] C.W. Therrien, *Discrete random signals and statistical signal processing*, Prentice Hall, 1992.